**Research paper**

# Evaluation of bearing capacity of multi-span spandrel-braced stone arch bridge based on static load test

## Hongshuai Gao[1], Hourui Duan[2], Yue Sun[3], Jiashuo Jian[4], Jingyuan Zhang[5], Hongbo Liu[6]

**Abstract:** Stone arch bridge is an important type in the early bridge construction process because of its beautiful shape, material saving and economic rationality. However, stone material will deteriorate after long-term operation, which results in a decrease in strength and bearing capacity of stone arch bridge. The vehicle load is increasing at the same time. Therefore, accurate evaluation of bearing capacity of stone arch bridge is essential to ensure safety. In this article, a three-span open-spandrel stone arch bridge was taken as research object. Firstly, the bridge damages were investigated and analyzed in detail, and bridge service state was evaluated. Then, based on the evaluation results of disease damages and considering stone material deterioration, a refined finite element model of stone arch bridge was established to analyze bending moment, axial force, strain and deformation. Finally, static load test was carried out to test vertical deformation and stress of arch ring, horizontal displacement of pier, settlement of foundation and development of cracks. The results show that static load test is the most accurate method for evaluating bearing capacity of stone arch bridge. The evaluation accuracy of finite element model based on material correction is in the middle, and the evaluation accuracy of disease damage assessment is the worst. In practical work, bearing capacity of stone arch bridge can be evaluated by combining the three methods with high accuracy and comprehensive results.

**Keywords:** static load test, stone arch bridge, bearing capacity, assessment method, open-spandrel arch bridge

[1]PhD., Eng., School of Civil Engineering, Heilongjiang University, Harbin 150080, PR China, e-mail: hong-shuai.gao@hlju.edu.cn, ORCID: 0000-0002-9304-5966

[2]MSc., School of Civil Engineering, Heilongjiang University, Harbin 150080, PR China, e-mail: 2202534@s.hlju.edu.cn, ORCID: 0000-0002-4883-2557

[3]School of Civil Engineering, Heilongjiang University, Harbin 150080, PR China, e-mail: sunyuehd@126.com, ORCID: 0000-0001-6520-1776

[4]MSc., School of Civil Engineering, Heilongjiang University, Harbin 150080, PR China, e-mail: jjshlju@126.com, ORCID: 0000-0002-7189-6006

[5]PhD., Eng., lnstitute of Engineering Mechanics, China Earthquake Administration, Harbin 150080, China, e-mail: zhangjingyuan2022@126.com, ORCID: 0000-0002-8808-7598

[6]Prof., PhD., Eng., School of Civil Engineering, Heilongjiang University, Harbin 150080, PR China, e-mail: Hliu@hlju.edu.cn, ORCID: 0000-0002-9365-5641

# 1. Introduction

Arch bridge is an early form in the bridge history in the world. it is an important product of the development process of bridge construction [1]. China's economy was small and the traffic construction was in urgent need of development from 1950 to 1970, thus, stone arch bridge with low cost became one of the main types. Stone arch bridges were continuously constructed and construction technology made great progress, which laid an important role in the development of masonry arch bridges in China [2, 3].

Arch bridge damages are extremely serious, due to natural environment, overload, design and construction, natural disasters and other factors. Lateral cracks, longitudinal cracks, arch ring deformation and other phenomena are all signs of bridge damage [4]. Traffic volume and vehicle load are increasing with continuous development of economy, coupled with accumulation of natural aging and damage of structure, stone arch bridge appeared different degrees of damage, thus bearing capacity evaluation is particularly important.

Many scholars have carried out various studies on the detection technology and bearing capacity of existing stone arch bridges. The residual bearing capacity of masonry arch bridges can be evaluated by means of stress intensity factors in fracture mechanics. Practical and effective calculation methods are proposed [5]. Influence of damage on ultimate bearing capacity of masonry arch bridges by kinematic method and finite element model [6]. Non-smooth contact dynamics method of implicit discrete element method is used to analyze stability state of masonry arch bridge, which effectively reveals a variety of collapse failure mechanisms [7]. A refined finite element model is established to systematically analyze deformation and strength parameters of static load performance of stone arch bridge, which based on characteristics of material composition and considering nonlinearity of material [8]. Plane inclination of stone arch bridge has a certain influence on its bearing capacity. Bearing capacity and damage condition of the main arch ring can be analyzed and evaluated by establishing analytical finite element models [9].

Non-stressing temperature and water content have a great influence on cyclic deformation and permanent deformation of stone arch bridge, which will lead to deterioration and aging of stone, stone joint cracking, and sidewall inclination. Tensile stress under temperature is the main reason for cracks. Witzany et al. [10] analyzed the foundation settlement and rotation effect under flood, and they also obtained the collapse probability of stone arch bridge under extreme flood. Geometric shape and abutment displacement have a great influence on stress of stone arch bridge. The decrease of arch axis will lead to increase of ultimate load, and the increase of arch axis will lead to decrease of ultimate load. Mechanism of displacement on collapse is analyzed [11]. A nonlinear finite element model for progressive collapse of stone arch bridges can be established by using contact algorithm combined with element inactivation technique. Strong and vulnerable regions of arch bridges are determined by using the concept of generalized stiffness [12]. After many years of use, material properties of stone arch bridge have different degrees of degradation.

In this paper, a three-span open-web stone arch bridge that has been used for more than 20 years is taken as an engineering example. Firstly, this bridge is tested on the spot to find

out current diseases and damages. the service condition of this bridge is evaluated based on the specification. Then, finite element software abaqus is used to establish analysis model. Considering influence of material aging, section reduction and load variation, the axial force, bending moment, stress and displacement are checked. All analyses are based on service limit state of bearing capacity and normal service limit state. Finally, according to the results of technical condition evaluation and finite element model calculation and analysis, static load test of this bridge is carried out. Vertical displacement and stress of arch ring, horizontal displacement of pier (abutment) and foundation settlement were tested, and cracks in the process of static load were observed. Bearing capacity was evaluated by comprehensive application of damage investigation and evaluation, finite element analysis and calculation, and static load test.

# 2. Project background

A bridge is located in Hengdaohe Town, Mudanjiang City, Heilongjiang Province, China. The total length of the bridge is 49.0 m, as shown in Fig. 1. This bridge structure type adopts an open-web stone slab arch. The bridge span is arranged as $3 \times 13.8$ m, rise-span ratio is 1/6, net span is 13.8 m, and net rise height is 2.3 m. The substructure adopts a gravity pier (platform) to expand the foundation. The bridge deck is arranged as 2.4 m carriageway and $2 \times 0.75$ m sidewalk, and full width of the bridge deck is 3.9 m. The bridge was completed in 1993 and has been used for more than 20 years, which poses a certain threat to safety. Bridge type layout and standard cross section are shown in Fig. 2. Due to lack of original design data, cross-sectional and longitudinal dimensions in the figure are the data obtained from actual measurement in the field.
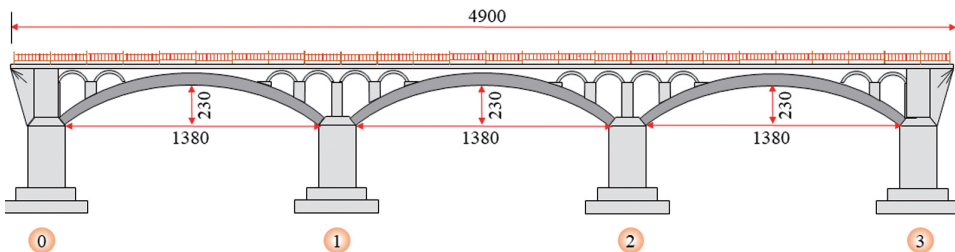


Fig. 1. Bridge photo



Fig. 2. Bridge layout

# 3. Investigation and evaluation of bridge damage

## 3.1. Damage investigation

According to the results of field observation, the damages of this stone arch bridges are summarized, and it is found that damages mainly occurred in the superstructure and substructure, and damages of the bridge deck system are less.

### 3.1.1. Superstructure

The main damages of superstructure are transverse cracks of abdominal arch, with the maximum width of 0.5 mm. There is mortar shedding, white phenomenon at the bottom of main arch ring, as shown in Fig. 3.
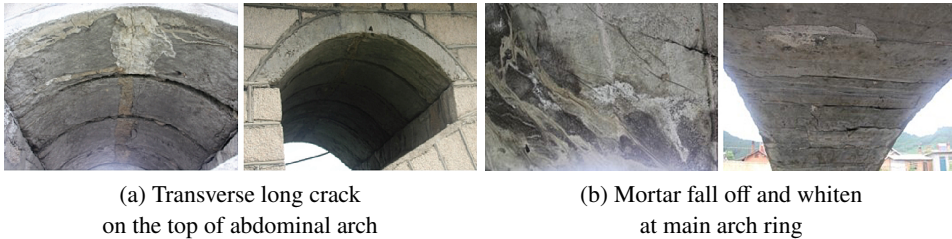


(a) Transverse long crack
on the top of abdominal arch

(b) Mortar fall off and whiten
at main arch ring

Fig. 3. Main damages of superstructure

### 3.1.2. Substructure

The main damages of substructure are pier scour, foundation scour and upstream riverbed deposition, as shown in Fig. 4.



(a) Pier scour                    (b) Foundation scour                    (c) Riverbed deposition

Fig. 4. Main damages of substructure

### 3.1.3. Bridge deck system

The main damages of bridge deck system are pits, mesh cracks and transverse penetrating cracks, as shown in Fig. 5.

(a) Transverse crack      (b) Mesh cracks      (c) Pits
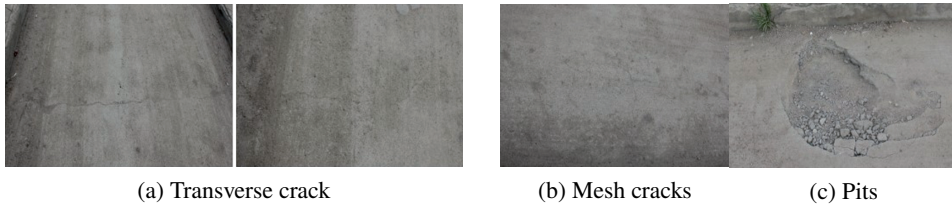
Fig. 5. Main damages of bridge deck system

### 3.1.4. Foundation

Since this arch bridge adopts natural expanded foundation, it needs to be examined in detail, as shown in Fig. 6, and geotechnical engineering investigation is carried out by drilling. The results show that change of foundation soil layer is complex, but there is no soft interlayer at the bottom of foundation, and natural foundation can be used. Round gravel, coarse sand and pebble layer can be used as the foundation bearing layer, and foundations are in good working conditions.



Fig. 6. Foundation conditions

## 3.2. Technical condition evaluation

The method in the "Standards for technical condition evaluation of highway bridges" (JTG/T H21-2011) [13] is used to evaluate the appearance damages of this bridge. The specific results are shown in Table 1. The superstructure includes main arch ring, arch

Table 1. Bridge technical status score

| No. | Bridge component | Weight | Component score | Bridge structure score |
|-----|------------------|--------|-----------------|------------------------|
| 1 | Superstructure | 0.40 | 56.48 | 22.59 |
| 2 | Substructure | 0.40 | 51.33 | 20.53 |
| 3 | Bridge deck system | 0.20 | 62.55 | 12.51 |
| Bridge score | | | | 55.63 |
| Classification of bridge technical conditions | | | | 4 |

superstructure and bridge deck. The substructure includes piers, abutments, foundations and riverbeds. The bridge deck system includes bridge deck pavement, railings and drainage systems. The comprehensive evaluation points of this bridge is 55.63, and the evaluation level is 4. So this bridge is in a dangerous state and needs to be overhauled or strengthened.

# 4. Calculation of bridge limit state

## 4.1. Calculation method of bearing capacity

According to the "Specifications for design of masonry and concrete highway bridges and culverts" (JTJ 022-85-1985) [14] and "Specification for Inspection and evaluation of load-bearing capacity of highway bridges" (JTG/T J21-2011) [15], the calculation is carried out. Bearing capacity assessment according to Highway Grade II Load (as shown in Fig. 7) load should meet the requirements of Eq. (4.1).

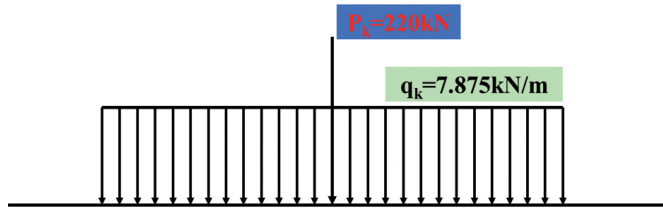$$(4.1) \qquad S_d \left( \gamma_{s0} \psi \sum \gamma_{s1} Q \right) \le R_d \left( R_j / \gamma_m, \alpha_k \right) Z_1 \left( 1 - \xi_e \right)$$



Fig. 7. Lane load of Highway Grade II Load

In Eq. (4.1), $S_d$ – load effect function; $Q$ – effect of load on structure; $\gamma_{s0}$, $\gamma_{s1}$ – importance coefficient and load safety coefficient of structure; $\psi$ – load combination factor; $R_d$ – effect function of structural resistance; $R_j$ – ultimate strength of masonry; $\gamma_m$ – safety factor of masonry; $\alpha_k$ – geometric dimension coefficient of structure; $Z_1$ – calculation coefficient of bearing capacity, and the value is 0.93; $\xi_c$ – section reduction coefficient, and the value is 0.931.

## 4.2. Load combination and structural analysis model

### 1. Load combination

Calculation of bridge, the most unfavorable combination of various loads according to Eq. (4.2).

$$(4.2) \qquad S = 1.2 \times S_G + 1.4 \times \xi_q S_Q$$

In Eq. (4.2), $S_G$ – dead-weight effect of structure; $S_{Q1}$ – vehicle load effect of structure; $\xi_q$ – vehicle load correction coefficient.

## 2. Structural analysis model

In this checking analysis, ABAQUS is used to establish a refined finite element model. The element type is C3D8R. Pier, abutment, foundation and main arch ring are jointly modeled as the main components, which are called main bearing capacity structure. Abdominal arch, abdominal arch pier and filler on the arch play the role of transferring load, which are called the accessory bearing capacity structure. The three parts are modeled separately and directly connected by "tie". "Tie" connection is also adopted between the main and accessory bearing capacity structures. Finite element model is shown in Fig. 8.
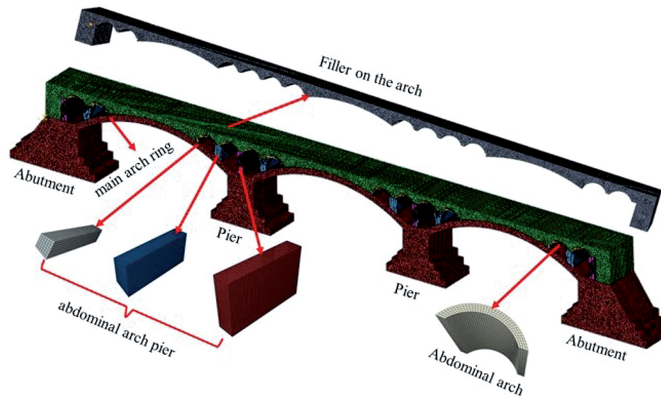


Fig. 8. Finite element calculation model

## 4.3. Calculation for ultimate limit state

### 4.3.1. Calculation of axial force

Axial force of the most unfavorable combination design value of main arch ring load effect is shown in Table 2. It can be seen that under highway-II load considering section reduction, axial force of each control section of main arch ring basically meets bearing

Table 2. Axial force calculation of main arch ring

| Control section | Axial force (kN) | Bearing capacity (kN) | Bearing capacity after section reduction (kN) | Bearing capacity after section reduction and mortar compression (kN) | Assessment |
|---|---|---|---|---|---|
| Arch footing | 2673 | 3207 | 2983 | 2386 | No |
| L/4 span | 2098 | 2517 | 2341 | 1873 | No |
| Midspan | 1086 | 1303 | 1211 | 969 | No |
| L/4 span | 2098 | 2517 | 2341 | 1873 | No |
| Arch footing | 2673 | 3207 | 2983 | 2386 | No |

capacity requirements. However, when both considering section reduction and mortar compression, axial force of each control section of main arch cannot meet bearing capacity requirements of highway-II.

### 4.3.2. Calculation of moment

Bending moment of the most unfavorable combination design value of main arch ring load effect is shown in Table 3. It can be seen that under the action of highway-II level load considering section reduction, bending moment of each control section of main arch ring basically meets bearing capacity requirements. However, when considering section reduction and mortar compression, bending moment of each control section of main arch can't meet bearing capacity requirements of highway-II.

Table 3. Moment calculation of main arch ring

| Control section | Moment (kN · m) | Bearing capacity (kN · m) | Bearing capacity after section reduction (kN · m) | Bearing capacity after section reduction and mortar compression (kN · m) | Assessment |
|---|---|---|---|---|---|
| Arch footing | −1102 | −1322 | −1230 | −984 | No |
| L/4 span | 723 | 868 | 807 | 645 | No |
| Midspan | 1382 | 1658 | 1542 | 1234 | No |
| L/4 span | 723 | 868 | 807 | 645 | No |
| Arch footing | −1102 | −1322 | −1230 | −984 | No |

## 4.4. Calculation for serviceability limit state

### 4.4.1. Calculation of stress

Prerequisite of continuous load, the calculated stress of each control section of main arch ring is shown in Table 4 (pressure is positive and tension is negative). It can be seen

Table 4. Stress calculation of main arch ring

| Control section | Location | Stress (MPa) | | Tensile design strength (MPa) | Compressive design strength (MPa) |
|---|---|---|---|---|---|
| | | no considering mortar compression | considering mortar compression | | |
| Arch footing | upper edge | 0.153 | 0.224 | 1.78 | 16.70 |
| | lower edge | −0.521 | −0.782 | 1.78 | 16.70 |
| Midspan | upper edge | −0.565 | −0.617 | 1.78 | 16.70 |
| | lower edge | 0.109 | 0.141 | 1.78 | 16.70 |

that the lower edge of arch footing section is tensioned and the upper edge is compressed, and the lower edge of the midspan section is compressed and the upper edge is tensioned, which can meet the requirements of highway-II load level.

### 4.4.2. Calculation of deflection

The deflection control section can be selected L/4 span section. When vehicle load is applied to the bridge deck, sum of the maximum absolute value of the positive and negative deflection of arch ring is less than L/800. Deflection calculation results are shown in Table 5, the sum of the absolute value is less than allowable value of specification, which meets the requirements of highway-II load grade.

Table 5. Deflection calculation of main arch ring

| Control section | Maximum deflection (mm) | Minimum deflection (mm) | Sum of absolute deflection (mm) | Specification allowable value (mm) |
|---|---|---|---|---|
| L/4 span | 2.02 | –0.24 | 2.26 | 17.8 |

Through analysis of ultimate limit state and normal serviceability limit state, it can be found that axial force and bending moment do not meet the requirements, but stress and deflection can meet the requirements. The static load test can evaluate the bearing capacity of the structure by applying the static load at the designated position of the bridge, testing the parameters such as strain and deflection of the key section, and comparing the test results with the theoretical value. Therefore, it is necessary to carry out static load test to further determine bearing capacity of the bridge.

# 5. Static load test results and discussion

## 5.1. Design of static load test scheme

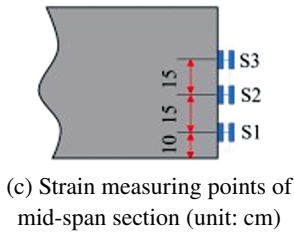### 5.1.1. Arrangement of testing points

This bridge has three spans. The first span is selected for static load test. The arrangement of displacement, strain and foundation settlement measuring points is shown in Fig. 9. D1~D5 are the vertical displacement measuring points of mid-span section, H1~H4 are the horizontal displacement measuring points of arch footing section, C1 is the foundation settlement measuring point, S1~S5 are the strain measuring points of mid-span and arch footing section. Displacement and settlement are measured by dial indicator with accuracy of 0.01 mm, and strain is measured by dial indicator with accuracy of 0.001 mm, as shown in Fig. 10.
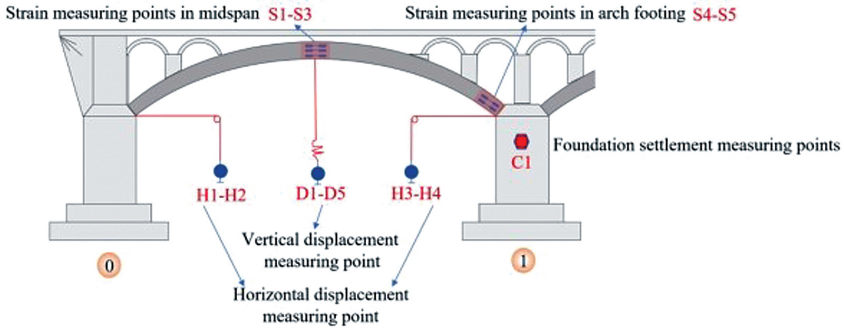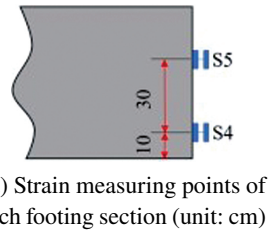
(a) Longitudinal layout of measuring points



(b) Displacement measuring points on bottom face



(c) Strain measuring points of
mid-span section (unit: cm)



(d) Strain measuring points of
arch footing section (unit: cm)

Fig. 9. Arrangement of measuring points in static load test



(a) Vertical displacement measurement



(b) Horizontal displacement measurement



(c) Settlement measurement



(d) Strain measurement

Fig. 10. Displacement and strain measurement

### 5.1.2. Determination of test vehicle

In order to simulate the maximum bending moment effect and ensure static test effectiveness, a 211.0 kN heavy vehicle was selected as test load in this test. Highway-II load was simulated by changing longitudinal position of bridge deck to ensure test load efficiency. The schematic diagram of test vehicle is shown in Fig. 11. The information of axle load and axle distance of this vehicle is shown in Table 6.
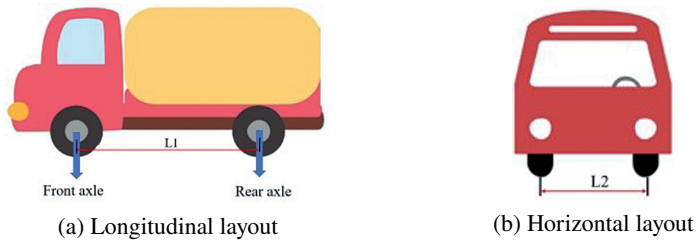


(a) Longitudinal layout  (b) Horizontal layout

Fig. 11. Loading vehicle diagram

Table 6. Axle load and axle distance information of load vehicle

| Front axle load (kN) | Rear axle load (kN) | Total weight (kN) | Longitudinal axial distance L1 (m) | Horizontal axial distance L2 (m) |
|---|---|---|---|---|
| 70.3 | 140.7 | 211.0 | 3.2 | 1.8 |

### 5.1.3. Test conditions and load arrangement

Vehicle load is arranged according to "General Code for Design of Highway Bridges and Culverts" (JTJ D60-2004) [16], and the most unfavorable load is arranged longitudinally according to the bending moment influence line of each section. The bending moment influence line of each section is shown in Fig. 12 and Fig. 13.
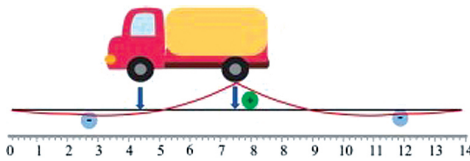


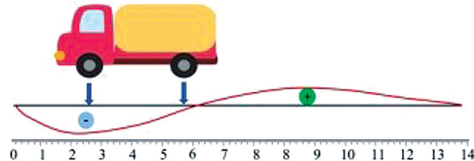Fig. 12. Influence line of bending moment in midspan

Fig. 13. Influence line of bending moment in arch footing

In order to simulate the maximum load effect of highway-II level, longitudinal position of test vehicle on bridge deck is changed to ensure that load efficiency is within specified range. It is divided into three conditions.

Condition 1: The rear axle of test vehicle is arranged in the middle of the span, the stress, the vertical displacement of midspan section and the horizontal displacement of pier are tested.

Condition 2: The rear axle of test vehicle is arranged at 2 m from the center line of pier, the stress of arch footing section and the horizontal displacement of pier are tested.

Condition 3: The rear axle of test vehicle is arranged on the top of pier 1, and the foundation settlement is tested.

Loading arrangement of the above three conditions is shown in Fig. 14, and the actual loading photographs are shown in Fig. 15.
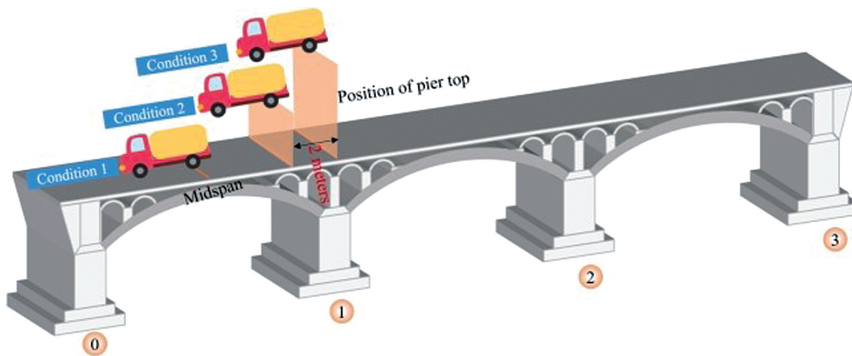


Fig. 14. Vehicle loading diagram



(a) Longitudinal loading　　　(b) Transverse loading　　　(c) Transverse loading
　　　　　　　　　　　　　　　　　(front view)　　　　　　　　　(back view)

Fig. 15. Photographs of actual vehicle loading

### 5.1.4. Efficiency of static load test

Static test load is determined according to the principle of equivalent control internal force. The efficiency of static load test can be calculated according to Eq. (5.1), which should be between 0.95 and 1.05.

(5.1)
$$\eta_q = \frac{S_s}{S'(1 + \mu)\eta_q}$$

In Eq. (5.1), $S_s$ – the maximum calculation effect value of internal force of loading control section corresponding to a loading test project under static test load; $S'$ – calculation value of the most unfavorable effect of internal force of the same loading control section generated by the highway-II load; $\mu$ – impact coefficient values by specification; $\eta_q$ – load efficiency of static test.

This bridge is calculated according to highway-II level, and the test load efficiency is shown in Table 7.

Table 7. Calculation value and validity of loading test

| Position | Theoretical value (kN · m) | Experimental value (kN · m) | Load efficiency $\eta_q$ |
|---|---|---|---|
| Midspan | 101 | 104 | 1.03 |
| Archfooting | −125 | 126 | 1.01 |

According to "Specification for Inspection and evaluation of load-bearing capacity of highway bridges" (JTG/T J21-2011) [15], load efficiencies of mid-span section and arch foot section are in the range of 0.95~1.05, which indicates that the test load is sufficient.

## 5.2. Test results and discussion

In bridge static load test, structural verification coefficient and residual coefficient are important index to evaluate bridge structural safety and determine bearing capacity. Generally, it is required that coefficient value is not greater than 1 [15]. The smaller the coefficient value is, the greater the structural safety reserve is. If coefficient value is too large or too small, the reasons should be analyzed from many aspects. For example, excessive coefficient value can indicate that structural material strength is low, connection of each structural part is poor or the stiffness is low. Small coefficient value indicates that strength and elastic modulus of material are high.

Structural verification coefficient $\zeta$ of static load test of main measuring points should be calculated according to Eq. (5.2).

$$(5.2) \qquad \zeta = \frac{S_e}{S_s}$$

In Eq. (5.2), $S_e$ – measured elastic displacements or strain values of main measuring points under test load; $S_s$ – theoretical calculation of displacement or strain values of main measuring points under test load.

Relative residual displacement or relative residual strain $S'$ of main measuring points should be calculated according to Eq. (5.3).

$$(5.3) \qquad S'_p = \frac{S_p}{S_t} \times 100\%$$

In Eq. (5.3), $S_p$ – measured residual displacement or residual strain values of main measuring points; $S_t$ – measured total displacement or total strain values of main measuring points under test load.

When one of the following situations occurs, it should be determined that bearing capacity does not meet the requirements.

    i. Structural verification coefficient of main measuring points is greater than 1.

    ii. The relative residual coefficient of main measuring points exceeds 20%.

    iii. The crack width exceeds the limit under test load, and the crack closure width is less than 2/3 of expansion width after unloading.

    iv. Unstable settlement displacement of bridge foundation occurs under test load.

### 5.2.1. Vertical displacement test results and analysis

Vertical displacement of midspan section is the largest under condition 1. Theoretical values, measured values and residual values of deflection of vertical displacement are listed in Table 8. Measured values and theoretical values are analyzed in detail, as shown in Fig. 16.
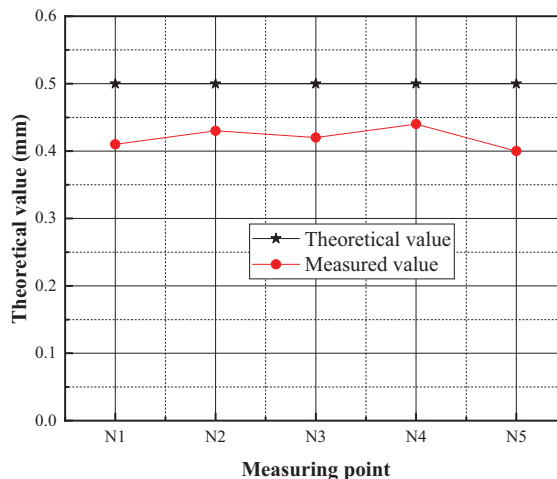


Fig. 16. Comparison of measured and theoretical values of mid-span section (condition 1)

Table 8. Comparison of measured and theoretical values of mid-span section (condition 1 unit: mm)

| Measuring point | D1 | D2 | D3 | D4 | D5 |
|---|---|---|---|---|---|
| Theoretical value | 0.50 | 0.50 | 0.50 | 0.50 | 0.50 |
| Measured value | 0.41 | 0.43 | 0.42 | 0.44 | 0.40 |
| Residual value | 0.02 | 0.01 | 0.03 | 0.04 | 0.02 |
| Residual coefficient | 5% | 2% | 7% | 1% | 5% |
| Verification coefficient | 0.82 | 0.86 | 0.84 | 0.88 | 0.80 |

It can be seen from Table 8 and Fig. 16 that under test load, displacement measured values of midspan section are less than theoretical values, indicating that structural stiffness meets the requirements. The maximum value of verification coefficient is 0.88, which meets the specification requirement of less than 1, indicating that this bridge capacity meets the requirements of highway-II load. The maximum residual coefficient is 7%, which is less than the specification value of 20%, indicating that this bridge has good elastic recovery ability.

### 5.2.2. Strain test results and analysis

According to loading conditions of each control section in this bridge structure, the strain values of each control section measured in static load test are strain increment values after loading. The strain increment values calculated by theoretical and measured are compared below. Negative strain values represent tension and positive strain values represent compression. Theoretical values, measured values and residual values of strain are listed in Table 9 and Table 10.

It can be seen from Table 9 and Table 10 that under the test load, strain verification coefficients of midspan section and arch footing section of main arch ring are 0.50–0.85, which are all less than 1, indicating that bridge structural strength can meet the requirements. Residual values and coefficients are both 0, indicating that structural strains can fully recover after unloading.

Table 9. Comparison of measured and theoretical strain values under condition 1 (unit: με)

| Section position | Midspan | | | Arch footing | |
|---|---|---|---|---|---|
| Measuring point | S1 | S2 | S3 | S4 | S5 |
| Theoretical value | 53 | 13 | −27 | 4 | −2 |
| Measured value | 45 | 10 | −20 | 2 | −1 |
| Residual value | 0 | 0 | 0 | 0 | 0 |
| Residual coefficient | 0% | 0% | 0% | 0% | 0% |
| Verification coefficient | 0.85 | 0.77 | 0.74 | 0.50 | 0.50 |

Table 10. Comparison of measured and theoretical strain values under condition 2 (unit: με)

| Section position | Midspan | | | Arch footing | |
|---|---|---|---|---|---|
| Measuring point | S1 | S2 | S3 | S4 | S5 |
| Theoretical value | −9 | −2 | 4 | −48 | 24 |
| Measured value | −6 | 1 | 3 | −30 | 13 |
| Residual value | 0 | 0 | 0 | 0 | 0 |
| Residual coefficient | 0% | 0% | 0% | 0% | 0% |
| Verification coefficient | 0.67 | 0.50 | 0.75 | 0.62 | 0.54 |

### 5.2.3. Horizontal displacement test results and analysis

Because arch bridge is a structure with thrust, horizontal displacement of arch foot is a common phenomenon due to pier excessive thrust. Horizontal displacement of arch foot is generally accompanied by vault subsidence. Horizontal displacement of arch foot has a great influence on stress of arch bridge structure, and excessive displacement will cause cracks and other damages. For hingeless arch bridge with statically indeterminate structure, horizontal displacement of arch foot will produce redundant force in the elastic center of arch ring, as shown in Fig. 17.
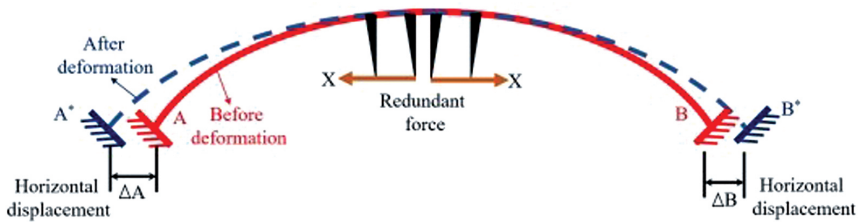


Fig. 17. Diagram of arch foot displacement

Therefore, it is very important to test horizontal displacement of pier. Test results are shown in Table 11. It can be seen that horizontal displacement is very small, and the pier has strong ability to resist horizontal thrust, which has no effect on each section stress of main arch ring.

Table 11. Measured values of horizontal displacement (unit: mm)

| Condition | Measuring point | S1 | S2 | S3 | S4 |
|---|---|---|---|---|---|
| Condition 1 | Measured value | 0.01 | 0.02 | 0 | 0.01 |
| | Residual value | 0 | 0 | 0 | 0 |
| Condition 2 | Measured value | 0 | 0.01 | 0 | 0.01 |
| | Residual value | 0 | 0 | 0 | 0 |

### 5.2.4. Foundation settlement test results and analysis

The test data of foundation settlement are shown in Table 12. It can be seen that there is no settlement in the loading process of pier foundation, indicating that foundation bearing capacity are good.

Table 12. Measured values of foundation settlement (unit: mm)

| Measuring point | C1 |
|---|---|
| Measured value | 0 |
| Residual value | 0 |

### 5.2.5. Experimental phenomena in loading process

There is no abnormal noise in this bridge under different loading conditions. Before and after loading, no new cracks appear in the main arch ring, and the original cracks can be fully recovered after unloading.

Through comprehensive analysis of the displacement and strain of midspan section, the displacement and strain of arch foot section, horizontal displacement of pier, foundation settlement and loading test phenomenon, it can be seen that bearing capacity of this bridge meets the requirements of highway-II load.

### 5.2.6. Discussion

The arch bridge assessment results are listed in Table 13, which based on damage assessment, finite element analysis and static load test. It can be found that static load test can accurately determine bearing capacity of arch bridge.

Table 13. Comparison of evaluation results

| No. | Assessment method | Assessment result | Feature |
|---|---|---|---|
| 1 | Damage assessment | In a dangerous state, and repair or reinforcement is required | Easy to implement, but inaccurate results |
| 2 | Finite element analysis | Axial force and bending moment do not meet the requirements, but stress and deflection meet the requirements | The safety state cannot be evaluated completely and accurately, which needs further evaluation. |
| 3 | Static load test | Carrying capacity meets the requirements | The assessment results are accurate, but on-site tests are needed and time and money are spent |

# 6. Conclusions

Based on the background of a stone arch bridge in Mudanjiang City, Heilongjiang Province, China, this paper conducts a qualitative and quantitative evaluation of the stone arch bridge. The following conclusions can be obtained.

1. The main damages of stone arch bridge are abdominal arch cracks, main arch mortar shedding and whitening, pier scouring, bridge deck pits and cracks. Foundation conditions are good. According to damage assessment, the stone arch bridge is classified into four categories and is in a dangerous state.

2. Finite element method is used to analyze ultimate capacity limit state and serviceability limit state of stone arch bridge. It is found that axial force and bending moment do not meet the requirements, but stress and deflection meet the requirements. Safety condition cannot be accurately assessed.

3. Static load test measured vertical displacement and strain of main arch ring, horizontal displacement of pier and foundation settlement. It is found that measured values of each point are less than theoretical calculation value, and stone arch bridge are in a safe working state.

4. The results of static load test can correspond to damage investigation of stone arch bridge, mainly reflecting that deformation and strain of main arch ring are small and main arch ring does not appear cracks. Horizontal displacement of pier and settlement of the foundation meet the requirements and foundation conditions are better corresponding.

5. Damages evaluation, finite element analysis and static load test can be used to evaluate stone arch bridge, but the static load test is the most accurate.

In practical engineering, in order to evaluate the reliability of stone arch bridges from different aspects, the conclusions in this paper can be used as a reference during the inspection of stone arch bridges.

# References

[1] T. Siwowski, H. Zobel, T. Al-Khafaji, W. Karwowski, "The recently built Polish large arch bridges - a review of construction technology", *Archives of Civil Engineering*, 2020, vol. 66, no. 4, pp. 7–43; DOI: 10.24425/ace.2020.135207.

[2] L. Ying, T. Huancheng, *Research on Chinese Stone Arch Bridges*. Beijing, China: China Communications Press, 1993.

[3] T. Yunyue, *China Stone Bridge*. Hunan, China: Hunan Education Press, 2002.

[4] J. Haifei, *Disease analysis and reinforcement method research of dangerous and old stone arch bridges on highways*. Chongqing Jiaotong University, 2010; DOI: 10.7666/d.y1694555.

[5] R. Panian, M. Yazdani, "Estimation of the service load capacity of plain concrete arch bridges using a novel approach: Stress intensity factor", *Structures*, 2020, vol. 27, pp. 1521–1534; DOI: 10.1016/j.istruc.2020.07.055.

[6] T. Kamiński, J. Bień, "Application of Kinematic Method and FEM in Analysis of Ultimate Load Bearing Capacity of Damaged Masonry Arch Bridges", *Procedia Engineering*, 2013, vol. 57, pp. 524–532; DOI: 10.1016/j.proeng.2013.04.067.

[7] A. Rafiee, M. Vinches, "Mechanical behaviour of a stone masonry bridge assessed using an implicit discrete element method", *Engineering Structures*, 2013, vol. 48, pp. 739–749; DOI: 10.1016/j.engstruct.2012.11.035.

[8] C. Costa, A. Arede, M. Morais, A. Anibal, "Detailed FE and DE Modelling of Stone Masonry Arch Bridges for the Assessment of Load-carrying Capacity", *Procedia Engineering*, 2015, vol. 114, pp. 854–861; DOI: 10.1016/j.proeng.2015.08.039.

[9] W. Bai, Y. Li, Q. Xie, "Numerical Simulation of Stone Arch Bridge Considering the Influence of Out-of-plane Tilt", *Journal of Beijing University of Technology*, 2016; DOI: 10.11936/bjutxb2015070023.

[10] J. Witzany, T. Cejka, R. Zigler, "Failure resistance of the historic stone bridge structure of Charles Bridge. I: Susceptibility to nonstress effects", *Journal of Performance of Constructed Facilities*, 2008, vol. 22, no. 2, pp. 71–82; DOI: 10.1061/(ASCE)0887-3828(2008)22:2(83).

[11] G.A. Drosopouios, G.E. Stavroulakis, C.V. Massalas, "Influence of the geometry and the abutments movement on the collapse of stone arch bridges", *Construction and Building Materials*, 2008, vol. 22, no. 3, pp. 200–210; DOI: 10.1016/j.conbuildmat.2006.09.001.

[12] Z. Xu, X. Lu, H. Guan, X. Lu, A. Ren, "Progressive-Collapse Simulation and Critical Region Identification of a Stone Arch Bridge", *Journal of Performance of Constructed Facilities*, 2013, vol. 27, no. 1, pp. 43–52; DOI: 10.1061/(ASCE)CF.1943-5509.0000329.

[13] National standards of the people's Republic of China, "Standards for Technical Condition Evaluation of Highway Bridges (JTG/T H21-2011)", China, 2011.

[14] National standards of the people's Republic of China, "Specifications for Design of Masonry and Concrete Highway Bridges and Culverts (JTJ 022-85-1985)", China, 1985.

[15] National standards of the people's Republic of China, "Specification for Inspection and Evaluation of Load-bearing Capacity of Highway Bridges (JTG/T J21-2011)", China, 2011.

[16] National standards of the people's Republic of China, "General Code for Design of Highway Bridges and Culverts (JTG D60-2004)", China, 2004.